Experimental hydration of natural volcanic clinopyroxene phenocrysts under hydrothermal pressures (0.5–3 kbar)⚲

FRANZ A. WEIS[1,2,*], ROLAND STALDER[3], AND HENRIK SKOGBY[1]

[1]Department of Geosciences, Swedish Museum of Natural History, Box 50007, SE-10405 Stockholm, Sweden
[2]Department of Earth Sciences, Uppsala University, Center of Experimental Mineralogy, Petrology and Geochemistry (CEMPEG), SE-752 36 Uppsala, Sweden
[3]Institute for Mineralogy and Petrography, Innsbruck University, A-6020 Innsbruck, Austria

ABSTRACT

Water is a key parameter in mantle rheology, magma genesis, magma evolution, and resulting eruption styles, because it controls the density and the viscosity, as well as the melting and crystallization behavior of a melt. The water content in nominally anhydrous minerals (NAMs) such as clinopyroxene recently has been used as a proxy for magmatic water contents. NAMs, however, may dehydrate during magma degassing and eruption. We performed rehydration experiments on potentially degassed clinopyroxene phenocrysts from various volcanic settings. The experiments were conducted in hydrogen gas at 1 atm or hydrothermal pressures ranging from 0.5 to 3 kbar to test the incorporation of water into natural clinopyroxene under water fugacities similar to those in a volcanic system. Our results show a dependence of the water content in the clinopyroxene crystals with pressure as the phenocrysts begin to dehydrate upon lower water fugacities in the experiments. Water loss or gain in a crystal occurs according to the relatively fast redox-reaction $OH^- + Fe^{2+} \leftrightarrow O^{2-} + Fe^{3+} + \frac{1}{2} H_2$, which was confirmed by Mössbauer spectroscopy. The kinetics of this redox-process are independent of pressure and thus water fugacity. Water contents in rehydrated clinopyroxene crystals can be related to magmatic water contents at various levels in a volcanic system. Our results thus show that the water content in erupted clinopyroxene phenocrysts cannot be taken for granted to be representative of magmatic water contents prior to magma degassing. The conducted experiments indicate the simultaneous dehydration of clinopyroxene along with magma ascent and degassing. Rehydration experiments under hydrothermal pressures, however, may be able to reconstruct clinopyroxene water contents at crystallization prior to dehydration.

Keywords: NAMs, clinopyroxene, hydrogen, hydrothermal pressure, magmatic water content

INTRODUCTION

Water in nominally anhydrous minerals (NAMs) such as clinopyroxene and olivine is important for mantle rheology and storage of water in the mantle, as well as for estimation of the volatile content in erupted lavas (e.g., Wade et al. 2008; Hamada et al. 2011; Lloyd 2014; Weis et al. 2015). Hydrogen in clinopyroxene is incorporated in structural defects such as cation vacancies (e.g., Mg^{2+} vs. $2H^+$) and charge deficiencies (e.g., Si^{4+} vs. $Al^{3+} + H^+$) where it is bonded to oxygen and, regarded as an oxide component, can be expressed as water concentration. Various studies have shown that upon ascent from the mantle or during volcanic eruptions NAMs can dehydrate by hydrogen diffusion out of the crystals. Experiments have indicated that such dehydration mainly occurs according to the relatively fast and reversible redox reaction

$$OH^- + Fe^{2+} \leftrightarrow O^{2-} + Fe^{3+} + \frac{1}{2} H_2 \qquad (1)$$
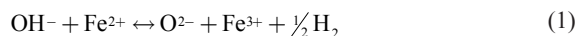
where the exchange of hydrogen ions (protons) is counter balanced by a flux of electron holes (e.g., Skogby and Rossman 1989; Skogby 1994; Bromiley et al. 2004; Koch-Müller et al. 2007; Sundvall and Skogby 2011). The kinetics of redox-reaction 1 in pyroxenes in particular have been well studied regarding hydration, dehydration, and dependence on iron content (Hercule and Ingrin 1999; Ingrin and Skogby 2000; Woods et al. 2000; Ingrin and Blanchard 2006; Stalder and Skogby 2007; Sundvall et al. 2009; Sundvall and Skogby 2011). Results from these studies demonstrate that hydrogen diffusion is strongly dependent on the Fe content and subsequent equilibration for clinopyroxenes with $X_{Fe/(Fe+Mg)} > 0.07$ occurs within days to minutes at temperatures from 600 to 1000 °C, with kinetics similar to those of hydrogen self-diffusion (H-D exchange; see reviews by Ingrin and Blanchard 2006 and Farver 2010). The hydrogen-associated defects in the crystal structure, however, will remain after the redox-dehydration since reaction kinetics for vacancy and cation diffusion are many orders of magnitude slower than the redox-processes (cf. Cherniak and Dimanov 2010). NAMs, especially clinopyroxene phenocrysts in mantle xenoliths or volcanic rocks, are therefore expected to keep a "memory" of their mantle hydrogen or the hydrogen content during original

crystallization from a magma. This difference in kinetics also has been exploited to rehydrate natural and synthetic clinopyroxenes by performing rehydration experiments in hydrogen gas at 1 atm and temperatures from 600 to 1000 °C (Skogby and Rossman 1989; Sundvall et al. 2009; Sundvall and Skogby 2011; Weis et al. 2015). Testing the same approach on fast erupted and partially dehydrated crystals from Tanganasoga volcano on El Hierro in the Canary archipelago, however, gave the indication that a full rehydration of the crystals was not possible at a pressure of only 1 atm. Water-rich clinopyroxenes from Tanganasoga actually lose parts of their water content during annealing experiments in H$_2$ atmosphere. Here we test the rehydration of Tanganasoga clinopyroxene crystals under pressures ranging from 0.5 to 3 kbar, which would better represent conditions within the upper part of a volcanic system. We further test this approach on a wider range of samples to study the rehydration process in a more general sense. Additional samples include clinopyroxene from basanite and ankaramite lavas from El Hierro and La Palma that were previously used for rehydration experiments at 1 atm to estimate magmatic water contents (cf. Weis et al. 2015). To get a comparison to clinopyroxene from Canary lava samples, clinopyroxene crystals of different composition and from various other rock types and volcanic environments on Earth and Mars are also included in the experiments.

SAMPLES

The majority of clinopyroxene crystals in this study come from the Canary Islands. More precisely, rock samples included are El Hierro island ankaramite lava vessels from Tanganasoga volcano and the Lomo Negro ankaramite lava flow (Carracedo et al. 2001; Longpré et al. 2009a; Villasante-Marcos and Pavón-Carrasco 2014). In addition, samples from basanite lava flows and one kaersutite cumulate xenolith from the 1971 Teneguia (Brändle et al. 1974) and 1949 Hoyo Negro (Klügel et al. 2000) eruptions on La Palma were included. To get broad comparisons regarding geological environments and chemical composition, additional clinopyroxene from the 2006 andesite lava from Merapi volcano (Gertisser 2001; Ratdomopurbo et al. 2013) on Java and basanite lavas from Shuangcai volcano in Zejiang prov-

ince, China (Liu et al., unpublished manuscript) were studied. Two further samples consist of a mantle xenolith from Kilbourne Hole, New Mexico (Kil and Wendlandt 2004; Harvey et al. 2012) and a specimen from the well-studied martian Nakhla meteorite (Bunch and Reid 1975; Treiman 1993). A full description of the samples used in this study is given in Table 1.

METHODS

Rock samples (n = 13) were crushed to obtain loose clinopyroxene crystals of a size suitable for analysis (≥300 µm). These were hand-picked under a binocular microscope and individual clinopyroxene crystals were then mounted in thermoplastic resin for further processing. With the help of crystal morphology and optical microscopy (extinction angles), the selected crystals (n = 37) were oriented along their crystallographic c-axis and their (100) and (010) crystal faces, on which the directions of the main refractive indices (α, β, and γ) occur. A detailed procedure of the crystal alignment is described in Stalder and Ludwig (2007). Various particle size-grades of Al$_2$O$_3$-grinding paper were used to thin and polish the oriented crystals to a thickness of a few hundred micrometers.

Electron probe microanalysis

Analyses of major elements (Al, Ti, Fe, Mg, Na, K, Si, Ca, Mn, Cr) in clinopyroxene crystals were carried out at the Department of Earth Sciences, Uppsala University, using a Field Emission-EPMA JXA-8530F JEOL hyperprobe. Between 5 and 8 spots were analyzed on each crystal using a beam current of 10 nA with an acceleration voltage of 15 kV with 10 s on peak and 5 s on lower and upper background. Standards used were fayalite (Fe$_2$SiO$_4$) for Fe, periclase (MgO) for Mg, pyrophanite (MnTiO$_3$) for Mn and Ti, corundum (Al$_2$O$_3$) for Al, wollastonite (CaSiO$_3$) for Ca and Si, eskolaite (Cr$_2$O$_3$) for Cr, nickel oxide (NiO) for Ni as well as albite (NaAlSi$_3$O$_8$), orthoclase (KAlSi$_3$O$_8$), and apatite Ca$_5$(PO$_4$)$_3$(OH,F,Cl) for Na, K, and P, respectively. Several crystals showed weak zonation in backscattered electron (BSE) images and for each crystal an average composition was calculated from all analyzed spots. A detailed description of the EPMA procedure and the analytical uncertainties is presented in Barker et al. (2015). From the obtained weight percentages, the number of atoms per formula unit in each crystal was calculated on the basis of a four cation-normalization. To distinguish between and quantify Fe^{2+} and Fe^{3+} in clinopyroxenes, Mössbauer spectroscopy was applied (see below). Average compositional data for clinopyroxene from samples LP1971-1, LP1949, and EH-Ank were taken from Weis et al. (2015).

Rehydration experiments

Experimental strategy. All rehydration experiments were performed at a temperature of 700 °C, at which hydrogen diffusion coupled to redox-reaction 1 has been shown to be active (Skogby and Rossman 1989; Skogby 1994; Stalder and Skogby 2003; Bromiley et al. 2004; Koch-Müller et al. 2007; Sundvall et al. 2009; Sundvall and Skogby 2011). Clinopyroxene crystals in this study show $X_{Fe/(Fe+Mg)}$

TABLE 1. Sample set used in this study

Sample	Description	No. of Cpx analyzed	Reference
Tanganasoga, El Hierro, Canary Islands			Carracedo et al. (2001); Longpre et al. (2009a)
T1	Ankaramite lava bomb	3	
T2	Ankaramite lava bomb	3	
T3	Ankaramite lava bomb	4	
T4	Ankaramite lava bomb	8	
Lomo Negro, El Hierro, Canary Islands			Villasante-Marcos and Pavón-Carrasco (2014)
EH-Ank	Ankaramite lava flow	3	
Cumbre Vieja Rift, La Palma, Canary Islands			Brändle et al. (1974); Klügel et al. (2000)
LP1971-B	Kaersutite cumulate xenolith, 1971 Teneguia eruption	4	
LP1971-1	Basanite lava, 1971 Teneguia eruption	1	
LP1949	Basanite lava, 1949 Hoyo Negro eruption	1	
Shuangcai volcano, Zejiang, China			Liu et al. (unpublished manuscript)
SC-1	Basanite lava, 5–10 Ma	4	
SC-2	Basanite lava, 5–10 Ma	4	
Merapi volcano, Java, Indonesia			Gertisser (2001); Ratdomopurbo et al. (2013); Troll et al. (2013)
MP-BA06-KA2	Basaltic andesite lava, 2006 eruption	5	
Kilbourne Hole, New Mexico, U.S.A.			Kil and Wendlandt (2004); Harvey et al. (2012)
KBH	Mantle xenolith	3	
martian meteorite			Bunch and Reid (1975); Treiman (1993)
Nakhla	Ultramafic cumulate, Mars	1	

> 0.08 (Table 2) and are thus above the threshold value suggested by Hercule and Ingrin (1999) ($X_{Fe/(Fe+Mg)} > 0.07$). Therefore, the hydration kinetics for Equation 1 are expected to be similar to the kinetics for hydrogen self-diffusion (Ingrin and Blanchard 2006). For rehydration it is also relevant how much Fe^{3+} is present in the crystals. Fe^{3+} generated by the redox-process discussed above would probably follow similar kinetics. Additional Fe^{3+} may have been incorporated during crystallization by other charge-balancing mechanisms such as an aegirine component ($NaFe^{3+}$). This Fe^{3+}, however, seems to be more stable and to take part in the redox-processes only in association with the occurrence of trivalent cations (e.g., Al^{3+}, Fe^{3+}) in the tetrahedral site, which are associated with hydrogen defects (Skogby and Rossman 1989; Skogby 1994; Purwin et al. 2009). However, a component involving ($NaFe^{2+}$) otherwise seems less likely. At 700 °C the reaction kinetics for hydrogen self-diffusion are as high as $-\log D = 11.3$ m²/s and hence at least 4.5 orders of magnitude higher than for vacancy diffusion ($-\log D \le 16$ m²/s) (Hercule and Ingrin 1999; Ingrin and Skogby 2000; Ingrin and Blanchard 2006; Cherniak and Dimanov 2010). Therefore, for the given temperature and time intervals, a relatively fast hydrogen diffusion is expected, whereas defects other than those generated by the redox-process are not expected to be significantly annealed. This is different to previous high-pressure and high-temperature experiments where the hydrogen solubility in clinopyroxene has been tested (e.g., Bromiley et al. 2004), where all structural defects are annealed. It is important to note that the experimental conditions did not intend to mimic conditions in a natural magmatic system, but simply to reverse redox-reaction 1.

The rehydration experiments were not buffered to control the oxygen fugacity. However, due to the hedenbergite component in the clinopyroxene crystals (see Table 2), we assume that the oxygen fugacity is controlled by the hedenbergite-magnetite-quartz buffer, which imposes redox conditions similar to QFM (cf. Gustafson 1974; Xirouchakis and Lindsley 1998). Water fugacities for pressure experiments behave in a linear relation to and do not deviate strongly from the nominal pressure (cf. Pitzer and Sterner 1994).

Rehydration at 1 atm. To rehydrate the defects in clinopyroxene that lost hydrogen during oxidation (see Eq. 1), the crystals were heated under a stream of H_2 gas for different time intervals (see Table 3 for details) at a temperature of 700 °C and an ambient pressure of 1 atm. The crystals were kept in a gold sample holder and placed into the middle of a horizontal glass-tube furnace after the target temperature had been reached. The temperature was measured with a $Pt_{100}-Pt_{90}Rh_{10}$ thermocouple placed directly above the samples, which has an estimated uncertainty of ±2 °C. Prior to the start of the hydrogen flow, the glass tube was flushed with CO_2 so that reaction between the minerals and ambient oxygen as well as an explosion-risk of the hydrogen gas was prevented. Clinopyroxenes were then heated. After thermal annealing, the glass tube was again flushed with CO_2 and the crystals were removed from the furnace. Heating and cooling times of the samples for this method are on the order of ~1 min.

Rehydration under pressure. For pressure experiments (Table 3), selected crystals were welded into Au-capsules with an outer (inner) diameter of 5.0 (4.6) mm together with 12 μL of water. To prevent any dissolution of the clinopyroxene during the experiments, about 2 mg of diopside powder ($CaMgSi_2O_6$) were added to the capsule. Au-capsules were sealed using a Lampert PUK U3 welding device (equipped with tungsten electrode, flushed with argon gas). Possible leaks causing water loss were identified by weighing the capsules before and after heating in an oven at 120 °C for 15 min. Pressure treatment was performed in Rene 41 steel-vessels in cold-seal pressure vessels at Innsbruck University using water as pressure medium. All experiments were performed at a temperature of 700 °C and pressures between 0.5 and 3 kbar (Table 3). The temperature was measured by Ni-CrNi thermocouples and pressures were measured with a Heise gauge and kept constant within 0.05 kbar during the whole run duration.

FTIR spectroscopy

Before and after thermal and/or hydrothermal treatment, polarized FTIR spectra in the range 2000–5000 cm⁻¹ were acquired on the oriented clinopyroxene crystals along the directions of the main refractive indices (α, β, and γ) to obtain the total absorbance: $A_\alpha + A_\beta + A_\gamma = A_{total}$. A_α and A_γ were measured on the (010) crystal face and A_β on (100). The polished crystals were measured in the sample compartment of a Bruker Vertex 70 spectrometer equipped with a NIR source (halogen lamp), a CaF_2 beamsplitter, a wiregrid polarizer (KRS-5), and an InSb detector. Another set of crystals was measured at Innsbruck University using a Bruker Hyperion 3000

TABLE 2. Major elements and normalized cations of clinopyroxenes used in this study obtained by electron probe microanalysis (EPMA)[a]

Sample	SiO₂	Al₂O₃	MgO	Na₂O	MnO	TiO₂	K₂O	CaO	FeO	Cr₂O₃	Total
T1 average	47.486	6.247	13.441	0.510	0.095	3.015	0.004	22.659	6.702	0.060	100.217
T2 average	47.662	6.527	13.412	0.513	0.097	3.121	0.003	22.600	6.678	0.066	100.679
T3 average	47.439	6.675	13.466	0.492	0.098	3.160	0.002	22.635	6.606	0.046	100.618
T4 average	47.951	6.418	13.662	0.475	0.125	2.979	0.005	22.571	6.594	0.056	100.838
EH-Ank average[b]	48.145	5.582	13.409	0.566	0.092	2.434	0.006	22.377	6.721	0.067	99.398
LP1971-B average	47.020	6.330	12.200	0.644	0.148	2.583	0.009	22.771	7.186	0.079	98.970
LP1971-1 average[b]	47.132	6.672	12.364	0.663	0.156	2.479	0.006	22.488	7.550	0.081	99.591
LP1949 average[b]	47.989	5.976	13.211	0.561	0.097	2.417	0.005	22.806	6.320	0.119	99.501
SC-1(1)	49.912	3.022	15.482	0.409	0.149	1.042	0.003	21.388	6.818	0.210	98.434
SC-2(1)	50.682	3.420	17.225	0.489	0.145	0.725	0.000	18.513	6.963	0.359	98.521
SC-2(2)	49.335	3.717	14.877	0.443	0.112	1.297	0.006	21.830	6.817	0.200	98.636
MP-3	51.202	2.378	14.976	0.347	0.610	0.471	0.002	20.936	8.490	0.012	99.425
MP-6	50.455	2.412	14.747	0.346	0.527	0.468	0.005	21.150	8.350	0.017	98.476
MP-7	51.238	2.398	15.078	0.328	0.495	0.443	0.007	21.024	8.308	0.017	99.337
MP-8	47.226	5.811	13.716	0.549	0.115	2.506	0.005	22.729	6.461	0.044	99.161
KBH Cpx	51.310	6.632	15.508	1.544	0.071	0.476	0.007	20.066	2.628	0.936	99.178
Nakhla Cpx	51.272	0.914	12.763	0.230	0.453	0.238	0.003	18.993	14.045	0.348	99.259

				Normalized cations							
Sample	Si⁴⁺	Al³⁺	Mg²⁺	Na⁺	Mn²⁺	Ti⁴⁺	K⁺	Ca²⁺	Fe²⁺	Fe³⁺	Cr³⁺	Total
T1 average	1.756	0.272	0.741	0.037	0.003	0.084	0.000	0.898	0.149	0.058	0.002	4.000
T2 average	1.755	0.283	0.736	0.037	0.003	0.086	0.000	0.892	0.138	0.068	0.002	4.000
T3 average	1.747	0.290	0.739	0.035	0.003	0.087	0.000	0.893	0.145	0.058	0.001	4.000
T4 average	1.761	0.278	0.748	0.034	0.004	0.082	0.000	0.888	0.134	0.069	0.002	4.000
EH-Ank average	1.794	0.245	0.745	0.041	0.003	0.068	0.000	0.893	0.129	0.079	0.002	4.000
LP1971-B average	1.767	0.280	0.683	0.047	0.005	0.073	0.000	0.917	0.138	0.088	0.002	4.000
LP1971-1 average	1.759	0.293	0.688	0.048	0.005	0.070	0.000	0.899	0.138	0.098	0.002	4.000
LP1949 average	1.785	0.262	0.733	0.040	0.003	0.068	0.000	0.909	0.099	0.097	0.004	4.000
SC-1(1)	1.865	0.133	0.862	0.030	0.005	0.029	0.000	0.856	0.173	0.040	0.006	4.000
SC-2(1)	1.878	0.149	0.951	0.035	0.004	0.020	0.000	0.735	0.174	0.041	0.010	4.000
SC-2(2)	1.843	0.164	0.828	0.032	0.003	0.036	0.000	0.874	0.172	0.041	0.006	4.000
MP-3	1.907	0.104	0.831	0.025	0.019	0.013	0.000	0.835	0.210	0.054	0.000	4.000
MP-6	1.896	0.107	0.826	0.025	0.017	0.013	0.000	0.852	0.209	0.054	0.001	4.000
MP-7	1.908	0.105	0.837	0.023	0.016	0.012	0.000	0.839	0.206	0.053	0.001	4.000
MP-8	1.759	0.255	0.762	0.040	0.004	0.070	0.000	0.907	0.160	0.041	0.001	4.000
KBH Cpx	1.864	0.284	0.840	0.109	0.002	0.013	0.000	0.781	0.068	0.012	0.027	4.000
Nakhla Cpx[c]	1.958	0.041	0.726	0.017	0.015	0.007	0.000	0.777	0.440	0.009	0.011	4.000

[a] Major elements are given in wt% oxide; [b] values taken from Weis et al. 2015; [c] Dyar (2003) (Mössbauer data).

TABLE 3. Results for annealing of clinopyroxene at 1 atm

Sample	Pressure (atm)	Time (h)	Water content (ppm weight H_2O)
T1(1)	1	0, 44, 60	672, 528, 553
T1(5)	1	0, 4, 8, 12, 26, 44, 60	790, 568, 557, 540, 538, 483, 482
T1(mös)[a]	1	0, 26	706, 493
T2(3)	1	0, 4, 8, 12, 26, 44, 60	569, 411, 474, 416, 420, 395, 402
T2(mös)	1	0, 26	701, 500
T3(1)	1	0, 4, 8, 12, 26, 44, 60	686, 536, 526, 533, 502, 483, 467
T3(3)	1	0, 26	987, 604
T3(4)	1	0.25, 0.5, 0.75, 1.5, 3	744, 717, 662, 642, 575, 565
T3(mös)	1	0, 26	659, 394
T4(2)	1	0, 4, 8, 12, 26, 44, 60	154, 173, 202, 214, 246, 253, 253
T4(5)	1	0, 110, 278	228, 288, 299
T4(5)	1	0, 26	971, 584
T4(6)	1	0, 16, 34	141, 232, 226
T4(mös)	1	0, 26	263, 307
EH-Ank(1)	1	0, 26	91, 241
EH-Ank(3)	1	0, 34, 60	81, 290, 326
EH-Ank(3)	1	0, 16, 44	670, 354, 298
LP1971-B (1)	1	0, 34	314, 434
LP1971-B (2)	1	0, 26	309, 409
LP1971-B (3)	1	0, 26	279, 406
SC-1(2)	1	0, 44, 60	84, 149, 164
SC-1(3)	1	0, 44, 60	239, 181, 182
SC-1(4)	1	0, 44, 60	137, 158, 142
SC-2(3)	1	0, 60	292, 173
SC-2(4)	1	0, 60	221, 183
KBH cpx2	1	0, 26, 44	565, 456, 454
KBH cpx3	1	0, 26	379, 379
MP-4	1	0, 26, 44	0, 146, 151
MP-5	1	0, 26, 44	0, 177, 177
Nakhla	1	0, 34	0, 16

Notes: For time intervals the value 0 refers to the starting value of the crystal prior to annealing. Estimated uncertainty for water contents is ±20%.
[a] The abbreviation (mös) refers to samples used for Mössbauer experiments.

microscope equipped with a Globar source, a KBr beamsplitter, and a MCT detector. Crystal thickness varied between 150 and 800 μm, with most crystals having a thickness between 200 and 400 μm for both the (100) and (010) orientations. Cracks and inclusions in the crystals were avoided by applying small apertures (100 to 400 μm) for masking during analysis. In some cases impurities (e.g., magnetite inclusions) were present in the beam path, but these appeared not to have had any significant effect on the OH range of the spectra. For each individual spectrum, 128 scans were performed and averaged. No significant differences between the analyses in the sample compartment and microscope measurements were observed. The obtained spectra were baseline corrected by a polynomial function and the individual OH bands were fitted with the software PeakFit and used for further calculations. The corresponding water contents were then calculated using both the wavenumber-dependent calibration function established by Libowitzky and Rossman (1997) and the mineral-specific (augite) calibration of Bell et al. (1995).

Mössbauer spectroscopy

The oxidation states of iron in clinopyroxenes before and, where possible, after the rehydration experiments were obtained by Mössbauer spectroscopy. To obtain a sample average for different iron valence states, powdered crystal separates were analyzed with a ^{57}Co standard source (active diameter 5.0 mm), while selected single crystals were analyzed using a point source (active diameter 0.5 mm) to investigate oxidation and reduction during rehydration experiments. Several powdered crystals (10 mg in total) from individual rock samples were mixed and ground with acrylic resin and pressed to a thin disk under mild heat (150 °C) for analysis with the standard source. Untreated, oriented single crystals for the point source were cut in half and one piece was used for rehydration experiments first. After the annealing and FTIR analysis the individual single-crystal pieces were powdered, mixed, and ground with thermoplastic resin and formed into a ~1 mm³ cylinder that was mounted on a strip of tape for analysis with the point source. The Mössbauer measurements were performed at incident angles of 90° and 54.7° to the γ-rays for the point and the standard source, respectively. All obtained spectra were calibrated against an α-Fe foil, folded and reduced from 1024 to 512 channels. The spectra fitting was done with the Mössbauer spectral analysis software MossA (cf. Prescher et al. 2012). During the fitting process, one doublet each was assigned to Fe^{2+} and Fe^{3+} in the octahedral positions. From the area of the doublets, the percentage of each oxidation state relative to the total iron content

of the sample was obtained, assuming similar recoil-free fractions for Fe^{2+} and Fe^{3+}. The estimated analytical error for the obtained Fe^{m+}/Fe_{tot} ratios is ±1%. No crystal-specific compositional analysis was carried out on the Mössbauer sample set due to the destructive nature of sample preparation. Mössbauer results for La Palma and El Hierro lava samples were taken from Weis et al. (2015). Data for the Nakhla meteorite were taken from Dyar (2003) due to the limited amount of sample material available.

RESULTS

Electron probe microanalysis

The clinopyroxene chemical data obtained by EPMA are shown in Table 2. The chemical composition of Tanganasoga clinopyroxenes was measured on a sample set separate to the one taken for rehydration experiments and is represented as average values. The full data set is available in Appendix[1] A1. The analyzed clinopyroxenes from the Canary Islands (n = 22) are all titanium-rich diopsides (2.5 to 3.3 wt% TiO_2) (Table 2, Fig. 1) with Mg# between 74 and 79 (mean = 78). With only very few exceptions, the individual crystals are homogeneous in composition and show limited zonation. Differences in chemical composition between crystals of individual rock samples occur on occasion. Clinopyroxenes from Merapi, Shuangcai, and Kilbourne Hole (n = 8) are also diopsides with Mg# from 76 to 82. The crystal from the Nakhla meteorite is an augite (Mg# = 62). The structural formulas for clinopyroxene phenocrysts from this study are reported in Table 2.

FTIR before rehydration

All analyzed clinopyroxenes showed absorption maxima at 3630, 3530, and 3460 cm⁻¹ in the IR spectra (Fig. 2), which corresponds to the typical vibrational bands expected for OH in diopside (e.g., Skogby 2006). The OH band at around 3630 cm⁻¹ is prominent for **E**∥α and **E**∥β, while the two bands around 3530 and 3460 cm⁻¹ dominate for **E**∥γ. This infrared-pleochroic behavior is typical for clinopyroxene OH bands (Fig. 2) (e.g., Beran 1976) and thus excludes the influence of possible OH-bearing impurities (e.g., hydrous minerals, melt/fluid inclusions).

Infrared analyses before rehydration experiments revealed a significant spread in the water content of the crystals from different rock samples (Table 3, Fig. 3). In some cases, water contents of clinopyroxene within individual rock samples varied significantly despite homogenous crystal chemistry. Water contents (given in parts per million weight H_2O) for clinopyroxene from Tanganasoga samples ranged from 141 to 790 ppm. Clinopyroxenes from the Lomo Negro and La Palma lava flows showed values between 36 and 364 ppm. Crystals from Merapi volcano were completely dry with water contents below detection limit, while those from Shuangcai volcano varied between 84 and 292 ppm. The crystals from mantle xenoliths from Kilbourne Hole showed values from 357 to 379 ppm. The martian clinopyroxene from the Nakhla meteorite was also completely dry with a water content below detection limit. Water contents corresponding to the spectra differed for the calibrations of Bell et al. (1995) and Libowitzky and Rossman (1997). Values determined with the mineral-specific calibration by Bell
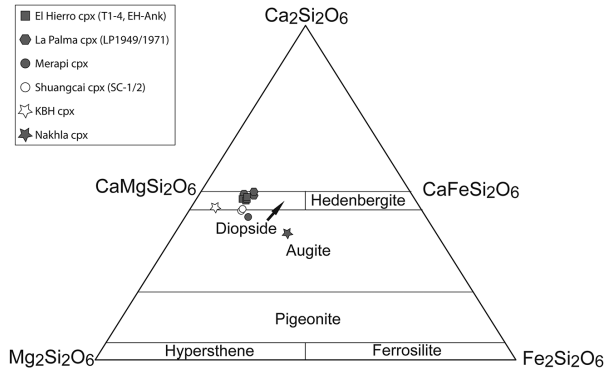
FIGURE 1. Compositional classification of clinopyroxenes shows most crystals from this study to plot in or close to the diopside field. Only Nakhla clinopyroxene has an augite composition (diagram after Morimoto et al. 1988).

et al. (1995) were about 25% higher, but the authors note that their mineral-specific (augite) calibration is primarily valid for samples with similar OH-spectra. Our diopside spectra mostly do not show a strong band at ~3460 cm^{-1} for $E\|\alpha$ and $E\|\beta$ and

thus differ from the spectra presented in Bell et al. (1995). We therefore used the values derived through the calibration by Libowitzky and Rossman (1997), which previously has been used successfully for synthetic as well as natural clinopyroxene samples (e.g., Stalder 2004; Stalder and Ludwig 2007; Sundvall and Stalder 2011) and that was reconfirmed by Mosenfelder and Rossman (2013).

Potential uncertainties for calculated water contents can arise from baseline correction and measurements of the crystal thickness. However, due to the quality of the spectra and the relatively large thickness of the crystals, a maximum error of ±10% is assumed for the precision of the calculated clinopyroxene water contents. In addition, the uncertainty regarding the accuracy of the values due to the calibration for absorption coefficients is another ±10% (cf. Libowitzky and Rossman 1997) resulting in an overall uncertainty of ±20% for the calculated clinopyroxene water contents. No hydrogen diffusion profiles were observed in the clinopyroxene crystals.

FTIR after rehydration at 1 atm. The thermal treatment caused no fractures or other visible effects on the crystals. The absorption bands increased significantly in height in all three directions (α, β, and γ) after thermal annealing in some samples
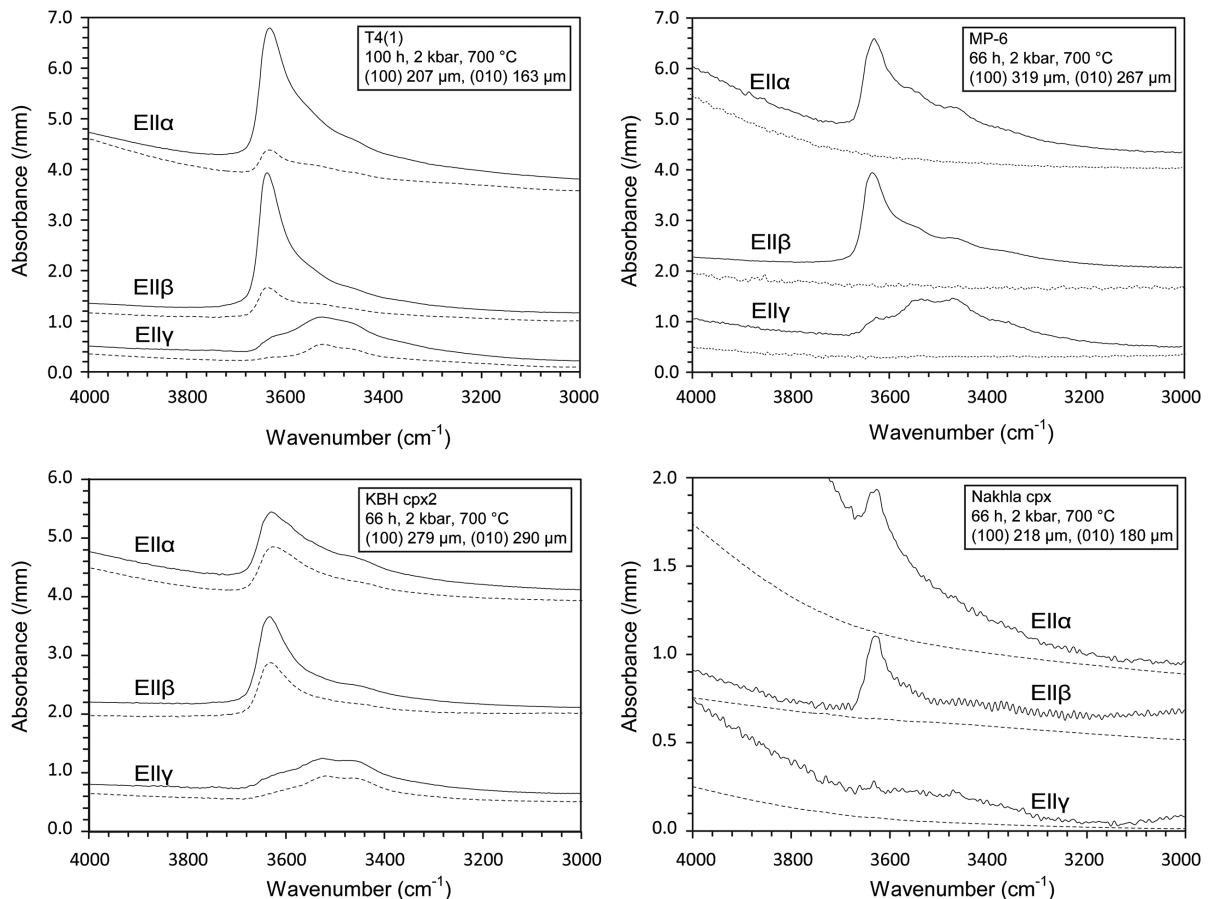

FIGURE 2. Representative IR spectra of clinopyroxene before (dashed line) and after (solid line) annealing at pressure. Polarized measurements with $E\|\alpha$ and $E\|\gamma$ were done on the (010) crystal face while $E\|\beta$ was measured on (100). Absorbances have been normalized to 1 mm thickness. The spectra show the three main vibrational bands of water at 3630, 3530, and 3460 cm^{-1}, which are expected for diopside (Skogby 2006) and relate to different OH-dipole orientations (see text for details). The increase in peak intensity and thus water content after pressure annealing is apparent.

while they decreased in others. The strongest increase as well as decrease in absorbance was notably always observed for the band at 3630 cm⁻¹. No change in band positions was observed, however. Treatment in H_2-atmosphere at 1 atm led to different hydration trends in clinopyroxene crystals from Tanganasoga. Water-poor crystals from sample T4 increased their hydrogen content to values between 226 and 307 ppm, whereas crystals with higher water contents from samples T1, T2, T3 (569 to 790 ppm) showed a decrease to hydrogen contents between 394 and 565 ppm. Clinopyroxene from Lomo Negro and the kaersutite cumulate xenolith from La Palma reached water contents between 241 and 434 ppm. The dry Merapi crystals increased to values between 151 and 177 ppm. Clinopyroxene from Shuangcai also showed a decrease as well as an increase in water contents with values between 142 and 183 ppm. One annealed crystal from Kilbourne Hole showed no significant change in water content. The Nakhla clinopyroxene increased to a water content of 16 ppm. Results for rehydration at 1 atm are presented in Table 3.

FTIR after rehydration under pressure. During the pressure experiments some crystals fractured along the cleavage planes and surfaces had to be re-polished. However, no entire crystal had to be discarded. Results for rehydration under pressure are presented in Table 4. Hydrothermal pressure annealing resulted exclusively in an increase in absorbance with the same pattern as for thermal annealing at 1 atm. All crystals seem to be close to saturation after 100–150 h of annealing, and no important changes within the analytical error of the water content occur or are to be expected. After pressure treatment Tanganasoga crystals reached water contents between 747 and 1129 ppm. Clinopyroxene from La Palma and Lomo Negro lava flows increased to values between 668 and 1180 ppm. Pressure-annealed clinopyroxene crystals from Merapi range between 712 and 794 ppm. Crystals from Shuangcai and

Kilbourne Hole revealed water contents between 425 and 704 ppm. The clinopyroxene from Nakhla showed a water content of 134 ppm after pressure annealing.

Hydrogen treatment of pressure-annealed samples. Several pressure-annealed clinopyroxene crystals from Tanganasoga [T3(3) and T4(5)], Lomo Negro (LN-3), and Kilbourne Hole (KBH-Cpx2) were again annealed at 1 atm and then showed a decrease in water content between 20 and 56%.

Mössbauer spectroscopy

The results for the Mössbauer spectroscopy of clinopyroxenes are shown in Tables 5 and 6. A representative spectrum with doublets for Fe^{2+} and Fe^{3+} is shown in Figure 4a. On average, the analyzed clinopyroxenes in this study show Fe^{3+}/Fe_{tot} ratios between 18 and 39%. Both reduction and oxidation of iron are observed upon hydrogen treatment (Table 6). Crystals that lost hydrogen during annealing showed an increase in Fe^{3+}/Fe_{tot} while those that incorporated hydrogen showed a reduction of the same. Neither metallic iron, which would indicate excessive reduction, nor oxidation products such as magnetite or hematite were observed after the experiments.

DISCUSSION

Redox processes

The variation in clinopyroxene water contents between individual rock samples, especially from the same location, correlates with the Mössbauer results. For example, clinopyroxene crystals in sample T4 from Tanganasoga show low water and higher Fe^{3+} contents than crystals from Tangansoga sample T1 where crystals have much higher water and lower Fe^{3+} contents. Mössbauer spectroscopy also shows that redox-reaction 1 was active during annealing experiments and Mössbauer data for the studied Tanganasoga crystals demonstrate reduction as well as oxidation of Fe^{3+} and Fe^{2+} after thermal annealing (Table 6). The increase and decrease of Fe^{3+} parallels the change in water
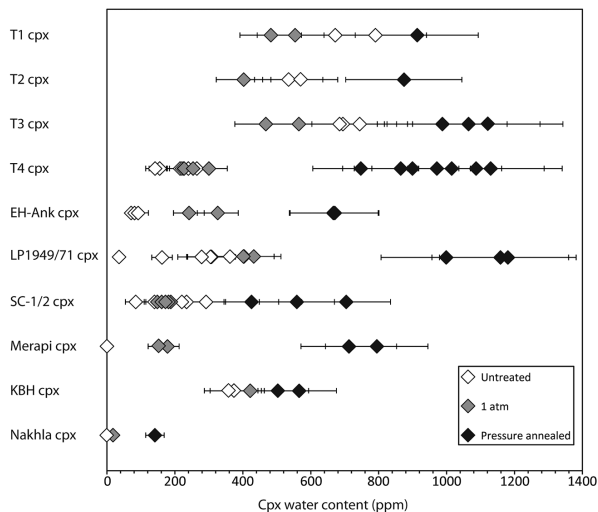
FIGURE 3. Distribution of measured water contents for clinopyroxene crystals from this study before and after thermal annealing at 1 atm and under pressure. Some crystals lose water upon treatment in hydrogen gas at 1 atm. Water contents increase drastically in all samples upon pressure annealing. Error bars represent the 20% uncertainty in the FTIR analysis.

TABLE 4. Results for pressure annealing of clinopyroxene

Sample	Pressure (kbar)	Time (h)	Water content (ppm weight H_2O)
T1(1)	2	0, 120	553, 912
T2(2)	2	0, 120	535, 874
T3(3)	2	0, 120	694, 1064
T3(3)	0.5	0, 46	1064, 987
T4(1)	2	0, 24, 60, 100	264, 696, 829, 899
T4(3)	0.5	0, 24,60,100	239, 545, 674, 747
T4(4)	2	0, 169	215, 1015
T4(5)	3	0, 24, 60, 100, 169	315, 797, 927, 1003, 1086
T4(5)	0.5	0, 72	1086, 971
T4(7)	2	0, 24, 60, 100	221, 949, 1019, 1129
EH-Ank(2)	0.5	0, 72	71, 668
EH-Ank(3)	2	0, 24	326, 670
LP1971-B (5)	2	0, 66	364, 1180
LP1971-1 (4)	2	0, 66	162, 1158
LP1949 (5)	2	0, 66	36, 998
SC-1(1)	2	0, 72	110, 425
SC-2 (1)	2	0, 72	193, 704
SC-2 (2)	0.5	0, 72	202, 559
MP-6	2	0, 66	0, 794
MP-7	2	0, 66	0, 712
MP-8	0.5	0, 72	0, 768
KBH cpx	2	0, 66	357, 503
KBH cpx2	2	0, 66	374, 565
Nakhla cpx	2	0, 66	16, 134

Notes: For time intervals the value 0 refers to the starting value of the crystal prior to annealing. Estimated uncertainty for water contents is ±20%.

TABLE 5. Mössbauer spectroscopy results

Sample	Int[a] (%)	FWHM (mm/s)	CS (mm/s)	DQ (mm/s)
T1				
Fe^{2+}	72.0	0.58	1.10	2.16
Fe^{3+}	28.0	0.47	0.53	0.59
T2				
Fe^{2+}	66.8	0.54	1.08	2.17
Fe^{3+}	33.2	0.47	0.54	0.59
T3				
Fe^{2+}	71.5	0.54	1.10	2.15
Fe^{3+}	28.5	0.44	0.54	0.58
T4				
Fe^{2+}	66.1	0.55	1.09	2.15
Fe^{3+}	33.9	0.49	0.53	0.59
LP1971-B				
Fe^{2+}	61.2	0.39	1.07	2.20
Fe^{3+}	38.8	0.34	0.50	0.61
SC-1				
Fe^{2+}	81.1	0.53	1.12	2.09
Fe^{3+}	18.9	0.44	0.50	0.61
SC-2				
Fe^{2+}	80.8	0.58	1.12	2.13
Fe^{3+}	19.2	0.43	0.51	0.62
MP-BA06-KA2				
Fe^{2+}	79.6	0.50	1.10	2.08
Fe^{3+}	20.4	0.36	0.53	0.58
KBH Cpx				
Fe^{2+}	85.5	0.56	1.15	2.12
Fe^{3+}	14.5	0.54	0.43	0.65

Notes: Int = intensity in percentage of total absorption area [a] = Fe^{m+}/Fe_{total}. FWHM = full-width at half maximum (including source width). CS = centroid shift. DQ = quadrupole splitting. Estimated uncertainty for intensities is ±1%.

content in the crystals (Fig. 5). Crystals that incorporated hydrogen under thermal annealing at 1 atm in hydrogen gas or under pressure annealing showed a reduction of Fe^{3+} and a decrease in Fe^{3+}/Fe_{tot}. The measured changes in Fe^{3+}/Fe_{tot} for the two investigated crystals from sample T4 match, within error, the expected changes in Fe^{3+}/Fe_{tot} based on the hydrogen incorporation during rehydration (Table 6). For example, crystal T4(7) incorporated 908 ppm of water upon thermal annealing, which corresponds to 0.022 atoms per formula unit (apfu). Considering the 1:1 ratio of redox-reaction 1 this intake would imply a reduction of 0.022 apfu Fe^{3+} corresponding to a change of 10.9% in Fe^{3+}/Fe_{tot} (Fe_{tot} = 0.203 apfu). Mössbauer analysis revealed a change in Fe^{3+}/Fe_{tot} of 9.2% (corresponding to 0.019 apfu). Those clinopyroxene crystals that showed a loss of hydrogen upon annealing at 1 atm revealed an increase in Fe^{3+}. The expected rise in Fe^{3+}/Fe_{tot}, matches again, within analytical error, the measured change in Fe^{3+}/Fe_{tot} obtained by Mössbauer spectroscopy. The minor discrepancies in expected vs. measured changes could be a consequence of small compositional differences between the investigated crystals and the sample average determined by EMPA. However, the results confirm that the hydrogen diffusion is linked to redox-reaction 1. Interesting is that hydrogen diffuses out of the clinopyroxene at 1 atm and that the charge-balancing oxidation of Fe^{2+} occurs despite the strongly reducing hydrogen atmosphere in the glass tube furnace. This implies that the hydrogen diffusion out of clinopyroxene crystals is not only

TABLE 6. Mössbauer spectroscopy results for hydration experiments

Sample	Int[a] (%)	FWHM (mm/s)	CS (mm/s)	DQ (mm/s)	$[H_2O]_{Cpx}$ (ppm)	$\Delta[Fe^{m+}]$ (%)	$\Delta[H_2O]_{Cpx}$ (ppm)	$\Delta[H_2O]_{Cpx}$ in (%) of Fe_{total}	$\Delta[H^+]_{Cpx}$ (apfu)	$\Delta[Fe^{3+}]$ (apfu)	Ratio[b]
T1 mös											
Fe^{2+}	67.5	0.61	1.17	2.02	706	−2.9 ± 2	−213	−2.5 ± 1.0	−0.005	0.006	0.9
Fe^{3+}	32.5	0.59	0.37	0.91		2.9 ± 2		2.5 ± 1.0			
T1 mös H_2											
Fe^{2+}	64.5	0.61	1.08	2.18	493						
Fe^{3+}	35.5	0.54	0.52	0.59							
T2 mös											
Fe^{2+}	65.9	0.65	1.09	2.13	701	−2.8 ± 2	−201	−2.4 ± 1.0	−0.005	0.006	0.9
Fe^{3+}	34.1	0.63	0.51	0.60		2.8 ± 2		2.4 ± 1.0			
T2 mös H_2											
Fe^{2+}	63.1	0.61	1.08	2.17	500						
Fe^{3+}	36.9	0.56	0.51	0.60							
T3 mös											
Fe^{2+}	67.7	0.57	1.16	2.02	659	−4.6 ± 2	−265	−3.2 ± 1.2	−0.007	0.009	0.7
Fe^{3+}	32.3	0.60	0.37	0.88		4.6 ± 2		3.2 ± 1.2			
T3 mös H_2											
Fe^{2+}	63.1	0.57	1.17	2.01	394						
Fe^{3+}	36.9	0.59	0.38	0.87							
T4 mös											
Fe^{2+}	61.7	0.60	1.08	2.19	263	1.7 ± 2	44	0.5 ± 0.2	0.001	−0.003	0.3
Fe^{3+}	38.3	0.57	0.51	0.62		−1.7 ± 2		−0.5 ± 0.2			
T4 mös H_2											
Fe^{2+}	63.4	0.60	1.08	2.19	307						
Fe^{3+}	36.6	0.60	1.08	0.62							
T4(7)											
Fe^{2+}	60.2	0.52	1.16	2.02	221	9.2 ± 2	908	10.9 ± 4.4	0.022	−0.019	1.2
Fe^{3+}	39.8	0.50	0.38	0.87		−9.2 ± 2		−10.9 ± 4.4			
T4(7) Pressure											
Fe^{2+}	69.0	0.54	1.11	2.17	1129						
Fe^{3+}	31.0	0.48	0.50	0.57							

Notes: Int = intensity in percentage of total absorption area. FWHM = full-width at half maximum (including source width). CS = centroid shift. DQ = quadrupole splitting. Δ = Estimated uncertainty for intensities is ±1%. $\Delta[Fe^{m+}]$ refers to the change in Fe^{m+}/Fe_{total} after annealing experiments. $\Delta[H_2O]_{Cpx}$ refers to the measured water loss or gain in crystals after annealing experiments. $\Delta[H^+]_{Cpx}$ refers to the loss or gain of hydrogen atoms in the investigated crystal. $\Delta[Fe^{3+}]$ refers to the change in Fe^{3+}/Fe_{total} after annealing experiments expressed in atoms per formula unit.
[a] Fe^{m+}/Fe_{total}.
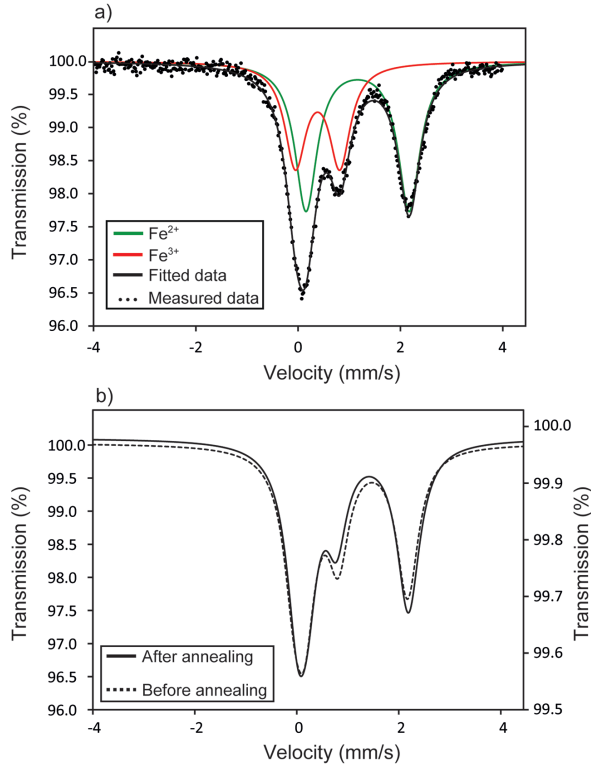[b] The ratio is given by $\Delta[H^+]_{Cpx}/\Delta[Fe^{3+}]$.

FIGURE 4. Representative Mössbauer spectra for clinopyroxene crystal T4(7) from Tanganasoga volcano. (**a**) Mössbauer spectrum of the sample before pressure annealing at 2 kbar and 700 °C. The spectrum shows the typical Fe^{2+} and Fe^{3+} doublets that were used to determine the concentration of both iron oxidation states in the crystal. (**b**) Comparison between the fitted lines before and after 100 h of pressure annealing. A decrease in Fe^{3+} after the annealing can be observed.

influenced by their environment (oxidizing vs. reducing) but is also pressure related.

De- and rehydration kinetics

Dehydration kinetics. Besides the obvious rehydration of crystals, a partial dehydration is observed when untreated crystals with higher water contents from Tanganasoga (>550 ppm) and Shuangcai (>220 ppm) or pressure-annealed crystals are treated in hydrogen gas at 1 atm. The dehydration commences almost immediately upon annealing (Table 3), although it seems to cease after about 40 h of annealing leading to a stabilization of the water content. Tanganasoga crystals dehydrate to values between 60 and 70% of the crystals' pre-annealing water content while Shuangcai crystals drop to values between 59 and 82%. This implies a dependence of the crystals' water contents on the prevailing water fugacity, and further supports previous conclusions that NAMs equilibrate their water content with varying fluid pressure (e.g., Hamada et al. 2011; Weis et al. 2015). Mössbauer data for Tanganasoga crystals (Table 5) show that this partial dehydration occurs by the oxidation of Fe^{2+} according to reaction 1. The oxidation takes place despite the reducing atmosphere provided by the hydrogen. The kinetics for hydrogen diffusion in and out of clinopyroxene have been well established

(Ingrin et al. 1995; Hercule and Ingrin 1999; Woods et al. 2000; Sundvall and Skogby 2011). The dehydration kinetics for clinopyroxene crystals annealed in hydrogen gas were tested in detail with two crystals from Tanganasoga sample T3. The two crystals were polished to a thickness of ~150 μm on the (010) crystal face and annealed at 700 °C for various time intervals (Table 7). From the results diffusion coefficients as previously described for one-dimensional diffusion through the two polished surfaces (cf. Carslaw and Jäger 1959; Ingrin et al. 1995) were calculated using Fick's seond law

$$\frac{c_t}{c_0} = \frac{8}{\pi^2} \sum_{n=0}^{\infty} \left(\frac{1}{(2n+1)^2} e^{\left(\frac{-Dt(2n+1)^2 \pi^2}{4L^2}\right)} \right).$$

Calculated diffusion curves are shown in Figure 6. The rate of diffusion for the dehydration along (010) is of the order $-\log D$ = 12.5 m²/s. Clinopyroxenes from Tanganasoga have $X_{Fe/(Fe+Mg)}$ > 0.21 and thus at the given temperature of 700 °C the expected value for $-\log D$ along (010) is 12.6 ± 0.4 m²/s (Hercule and Ingrin 1999; Woods et al. 2000). This shows that the pressure related dehydration at 1 atm within hydrogen gas occurs at similar kinetics as the hydrogen self-diffusion.

Rehydration kinetics. Similar as for the dehydration the results for the rehydration experiments can be used to calculate the kinetics according to the equation

$$\frac{c_t}{c_0} = 1 - \frac{8}{\pi^2} \sum_{n=0}^{\infty} \left(\frac{1}{(2n+1)^2} e^{\left(\frac{-Dt(2n+1)^2 \pi^2}{4L^2}\right)} \right).$$

Since the kinetics for rehydration at 1 atm are already well described (e.g., Hercule and Ingrin 1999; Sundvall et al. 2009; Sundvall and Skogby 2011) focus will be put on the rehydration under pressure. Plotting the diffusion curves for two crystals
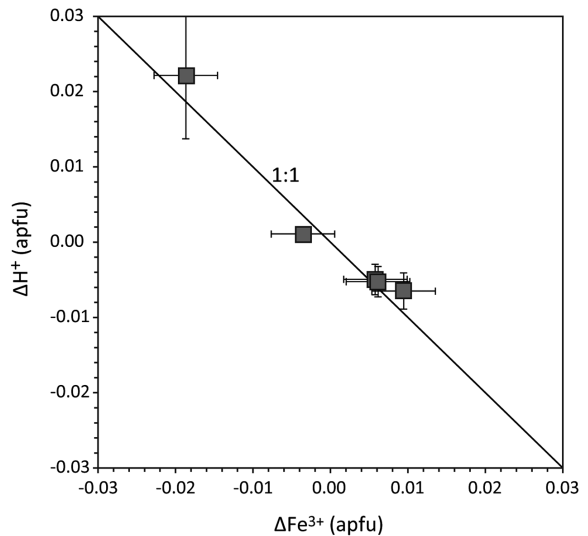

FIGURE 5. Correlation between hydrogen loss or gain and redox processes within clinopyroxene during annealing experiments. The change in Fe^{3+} and the loss or gain of hydrogen atoms in the clinopyroxenes follows almost perfectly the 1:1 relation proposed by redox-reaction 1 (see text for details).

TABLE 7. Clinopyroxene dehydration

Time (h)	T3(D2)		T3(D3)	
	$[H_2O]_{Cpx}$ (ppm)[a]	C_t/C_0[b]	$[H_2O]_{Cpx}$ (ppm)[a]	C_t/C_0[b]
0	382	1.00	469	1.00
0.13	376	0.98	422	0.90
0.25	370	0.97	418	0.89
0.75	345	0.90	450	0.96
1.5	333	0.87	391	0.83
3.5	320	0.84	358	0.76
9.5	279	0.73	324	0.69
26	278	0.73	328	0.70

[a] Concentration representative for (010), i.e., $A_\alpha + A_\gamma$.
[b] C_0 = starting value C_t = concentration after time t.

reveals values for $-\log D$ of 12.5 and 13.1 m²/s for (100) as well as 12.8 m²/s for (010) (Fig. 6). The values obtained for (010) are again similar to those for hydrogen self-diffusion at 700 °C and 1 atm considering analytical error. However, hydrogen self-diffusion along (100) under these conditions is supposed to occur at around $-\log D$ = 11.3 m²/s (Hercule and Ingrin 1999) and thus about one order of magnitude faster than calculated from our experimental data. Yet, the value of 12.5 m²/s is close to the diffusion of hydrogen along (100) with $-\log D$ = 13.1 ± 0.4 m²/s determined by Sundvall and Skogby (2011) during hydration experiments at 1 atm and 700 °C. Furthermore, Hercule and Ingrin (1999) report values between 12.8 and 13.7 m²/s for hydrogen extraction-incorporation processes in diopside, which is in good agreement with our obtained data.

Rehydration at different pressures

From the obtained data it is obvious that the rehydration under pressure results in higher water contents in the crystals than for annealing at 1 atm. A positive relation between pressure and clinopyroxene water content can be seen after the rehydration experiments (Fig. 7). The two crystals that have been subsequently annealed at lower pressures (2 and 3 kbar then at 0.5 kbar and finally at 1 atm) showed water loss. Plotting the water contents obtained for annealing experiments against the different pressures (1 atm to 3 kbar) on a logarithmic scale reveals a positive correlation. A perfect relation between pressure and water content cannot be seen for the total of the Tanganasoga crystals on first glance, which might be due to minor variations in crystal compositions (Tables 3 and 4). However, plotting the average water contents of annealed Tanganasoga clinopyroxene crystals for each pressure reveals a trend similar to that observed for the individual crystals. The same pressure relation is observed for clinopyroxene crystals from Shuangcai (sample SC-2). Samples from Lomo Negro and Merapi annealed at different pressures do not show this trend very clearly. For Lomo Negro crystals, which are very homogenous in composition, the trend still holds within the analytical error. The three Merapi crystals annealed at pressure, on the contrary, show differences in their compositions. Crystal MP-8 has significantly more tetrahedral Al^{3+} (Table 2), which is most likely the reason for the high water content at 0.5 kbar compared to the other crystals at 2 kbar.

Reconstruction of initial water contents in clinopyroxenes

Rehydration limitations. The hypothesis behind the rehydration of clinopyroxenes proposes that their "initial" water content, i.e., their equilibrium water content prior to possible dehydration,

can be restored. This previously has been tested in various studies with various different clinopyroxenes and annealing experiments conducted at 1 atm (Sundvall et al. 2009; Sundvall and Skogby 2011; Weis et al. 2015). It remains difficult to show to what extent the initial water content of the crystals can be reached by performing rehydration experiments. For example, de- and subsequent rehydration of synthetic iron-poor diopside showed that only ~75% of the crystal's initial water content could be restored (Sundvall et al. 2009). Despite this aspect of insufficient rehydration there might be also a risk of excessive hydration of the clinopyroxene crystals. Synthetic, originally dry but Fe^{3+}-rich clinopyroxene has been shown to incorporate substantial amounts of hydrogen upon annealing (Skogby 1994). Furthermore, due to fast ascent with limited to no magma degassing and violent eruption at Tanganasoga volcano (cf. Pinel and Jaupart 2000; Manconi et al. 2009; Stroncik et al. 2009; Pedrazzi et al. 2014), the clinopyroxene crystals from the pyroclastic material most likely were quenched. In this way, the crystals are expected to preserve their initial values (cf. Wade et al. 2008). Yet, our rehydration experiments exceed the water contents in untreated crystals, which might indicate an excessive hydration. Another issue is the possible effect that CO_2 and other volatiles might have on the water activity (e.g., Kovács et al. 2012; Yang et al. 2014) and thus on the rehydration of hydrogen-associated defects during the hydrothermal experiments. However, there are also arguments against insufficient as well as excessive rehydration.

The experiments, both de- and rehydration, conducted by Sundvall et al. (2009) on very iron-poor crystals were performed at much higher temperatures (1000 °C) on a timescale of several days. Due to much faster kinetics under these temperatures, vacancy and cation diffusion is much more likely and cannot be excluded. The hydrogen incorporation was not according to the 1:1 relation of redox-reaction 1 and despite the fact that more hydrogen was incorporated than Fe^{3+} was reduced, yet the original water content was not reached (Sundvall et al. 2009). Considering that the 1:1 relation thus was not followed during dehydration either, vacancy diffusion seems reasonable since the crystal otherwise would have been left without a charge balance upon complete dehydration. The vacancy diffusion also could explain hydrogen intake exceeding the Fe^{3+} reduction during rehydration. New defects such as vacancies incorporating hydrogen were generated; however, not so many that the initial water contents could be restored. Our crystals, on the contrary, are iron rich. Any dehydration could easily have been compensated by the oxidation of Fe^{2+}. Redox-processes in our experiment also follow more closely the 1:1 relation of reaction 1 (Fig. 5). In addition, experimental conditions in this study make cation and vacancy diffusion very unlikely.

The risk of an excessive rehydration may mostly be linked to the amount of Fe^{3+} available in the clinopyroxenes. The problem could be that additional available Fe^{3+}, which has not been linked to prior dehydration, is reduced and hydrogen incorporated. The hydration of initially dry, synthetic crystals by Skogby (1994) can be linked to the quantity of trivalent cations in the tetrahedral site. The hydrogen intake of the crystals equals almost 1:1 the amount of the latter (Skogby 1994). Mössbauer analysis further showed additional reduction of Fe^{3+}; however, no additional hydrogen intake occurred. Also, as pointed out previously, not
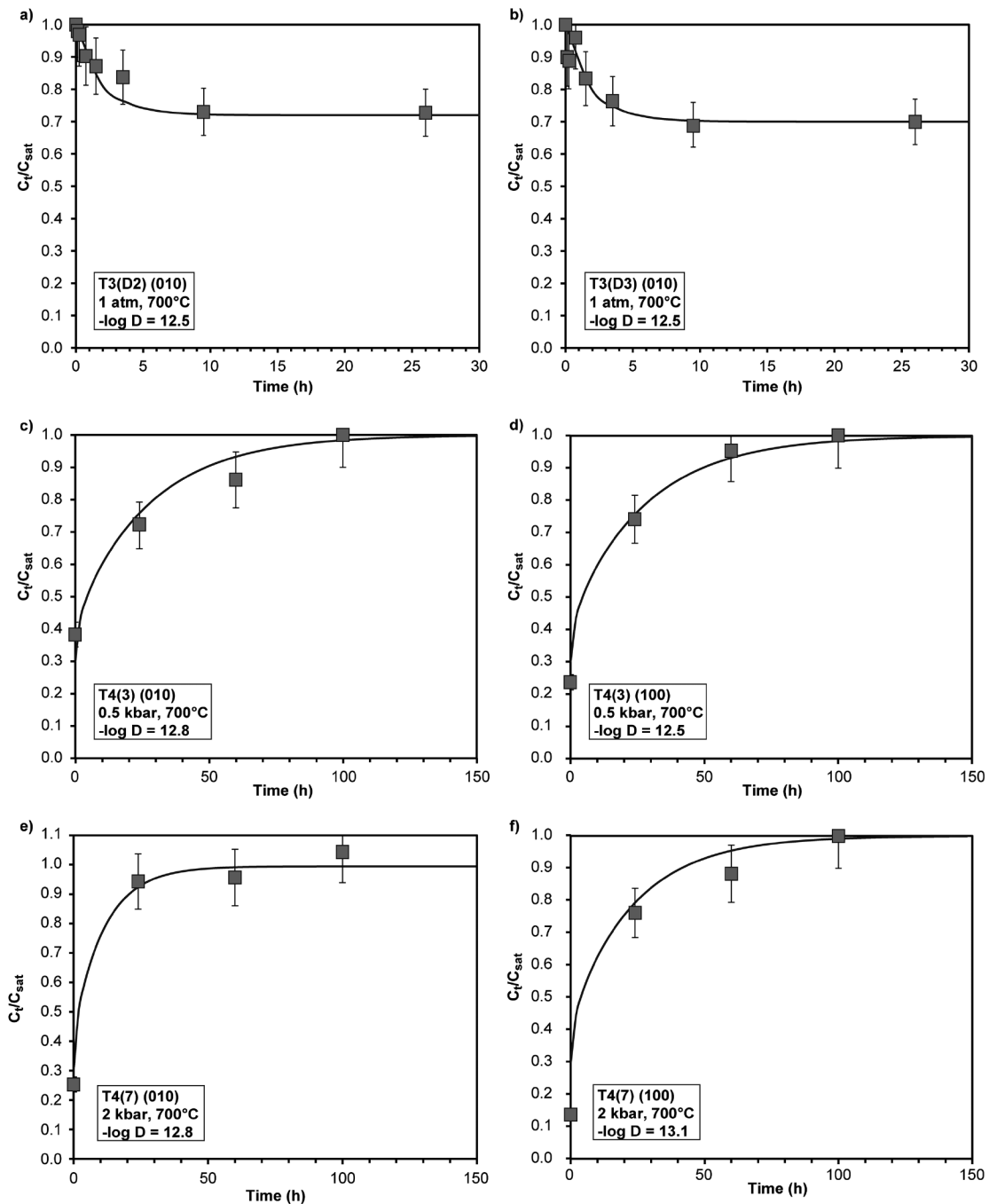
FIGURE 6. Diffusion curves for dehydration of clinopyroxene in hydrogen gas at 1 atm (**a** and **b**) and rehydration at different pressures (**c**, **d**, **e**, and **f**) at 700 °C. For **e**, the value for c_{sat} was taken as the average of the two highest concentrations in the crystal. Error bars represent the 10% error for the precision of the FTIR analysis. All values for $-\log D$ (D as m^2/s) fall within a narrow range and are similar to those obtained in previous studies (see text for details).

all Fe^{3+} in the clinopyroxene crystals can be reduced since some of it may be, for example, associated with an aegirine component that only favors a NaHFe^{2+} component in association with defects suitable for hydrogen incorporation (cf. Skogby and Rossman 1989; Purwin et al. 2009). Thus the defects become the limiting factor for the rehydration. Furthermore, the synthetic crystals in

Skogby (1994) were grown under dry conditions that, however, are very unlikely in a magmatic system.

The higher water contents in annealed Tanganasoga clinopyroxene compared to untreated crystals could be a consequence of minor degassing of Tanganasoga magmas and subsequent re-equilibration of the crystals to the new fluid pressure (e.g.,
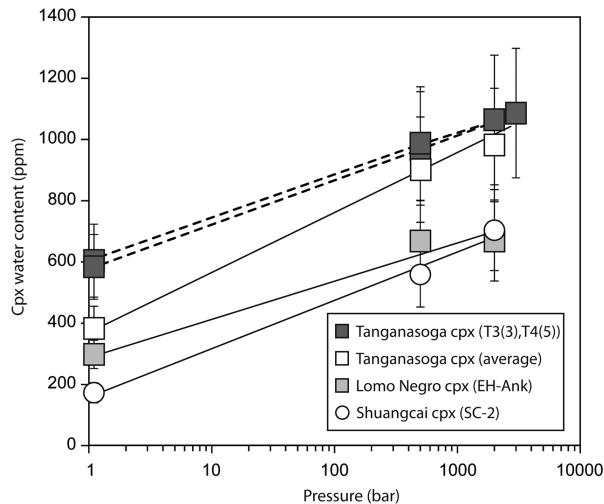
FIGURE 7. Relation between pressure and clinopyroxene water content. With increasing pressure, the water content in clinopyroxene crystals increases according to a logarithmic trend. Solid lines represent trends for crystal populations in individual rock samples. Dashed lines represent trends for individual crystals. Error bars represent the 20% error of the FTIR analysis.

Hamada et al. 2011). Our experiments show that pressure differences cause significant changes in clinopyroxene hydrogen content within a few hours. In addition, moderate dehydration by oxidation when exposed to the atmosphere prior to quenching of the clinopyroxenes during eruption can be assumed. Hydrogen diffusion in clinopyroxene is fast enough to evolve diffusion profiles over several millimeters within minutes at magmatic temperatures (cf. Woods et al. 2000; Lloyd 2014) and thus an effect of dehydration even on rapidly erupted crystals cannot be ruled out. Dehydration upon eruption may be indicated by the variation in clinopyroxene water contents (e.g., sample T2, $\Delta H_2O_{Cpx} > 120$ ppm) within individual rock samples despite homogenous crystal chemistry. Furthermore, pressure-annealed crystals from Shuangcai volcano reach water contents similar to the highest values reported in clinopyroxenes from Gaoping volcano in the Zhejiang province, China (Liu et al. unpublished manuscript) that are interpreted to have preserved more often their initial water content, in contrast to the samples from Shuangcai volcano where crystals are interpreted to have dehydrated.

Another issue regarding excessive hydration of the clinopyroxene crystals is the effect of CO_2 on the activity of water. It has been shown that other volatiles such as CO_2 or halogens within a magmatic system reduce the incorporation of hydrogen in NAMs (e.g., Stalder et al. 2008; Kovács et al. 2012; Yang et al. 2014). As such, the water contents in olivines annealed in a $H_2O + CO_2$ fluid phase, for example, were about half of those treated in pure H_2O (Yang et al. 2014). However, these studies concentrated on the solubility of hydrogen in NAMs, and the conducted experiments were done at pressures of several gigapascals and temperatures exceeding 1000 °C. Thus the annealed crystals experienced a resetting of their structural defects, and the influence of CO_2 on the generation of hydrogen-associated defects was tested. Experimental conditions in this study, however, do not intend a

reset of hydrogen associated defects but only a controlled reversal of redox-reaction 1 and thus a rehydration of already existing yet potentially dehydrated hydrogen-associated defects.

Furthermore, CO_2 activities in magmas from the Western Canaries might be low. Degassing of mostly CO_2-dominated fluids (~90%) commences at pressures above 1000 MPa in the upper mantle while most clinopyroxene crystallization is below this level (500 to 800 MPa) (e.g., Klügel et al. 2005; Longpré et al. 2008; Stroncik et al. 2009; Weis et al. 2015). Extensive degassing of H_2O might only occur upon slow magma ascent in the shallower, i.e., crustal, magma storage levels (e.g., Klügel et al. 2005; Longpré et al. 2008). A similar scenario may be the case for the Merapi clinopyroxenes. The main zone of clinopyroxene crystallization occurs between 300 and 600 MPa where most likely degassing of CO_2 and SO_2 from water-rich magmas occurs (Costa et al. 2013; Chadwick et al. 2013). Exsolution and degassing of water, on the contrary, has been modeled to commence below 300 MPa (Costa et al. 2013). Thus the influence of CO_2 on the crystals in this study may initially have been low. A precise effect of CO_2 or other volatiles on the rehydration experiments, however, is unknown and remains to be tested.

Corresponding magmatic water contents. It has been shown that the water content in clinopyroxene phenocrysts can be used to calculate the magmatic water content of their parent melt by applying appropriate crystal/melt partitioning data (Wade et al. 2008; O'Leary et al. 2010; Nazzareni et al. 2011; Okumura 2011; Xia et al. 2013; Weis et al. 2015; Liu et al., unpublished manuscript). This approach can be applied to test the validity of water contents in our rehydrated crystals. The presumption is that the magmatic water content determined through rehydrated clinopyroxenes correlates with values that are either observed or expected for the volcanic environment in which they crystallized.

For example, to determine parental magmatic water contents, Weis et al. (2015) performed rehydration experiments in hydrogen gas at 1 atm on clinopyroxenes from ankaramite and basanite lava flows from the Western Canaries. Applying the equation by O'Leary et al. (2010)

$$\ln D = -4.2(\pm 0.2) + 6(\pm 0.5)^{VI}[Al^{3+}] - 1(\pm 0.2)[Ca^{2+}]$$

and compositional data for clinopyoxene crystal/melt partition coefficients were calculated. From the partition coefficients and water contents of clinopyroxene after rehydration experiments, Weis et al. (2015) determined parental H_2O contents between 0.71 ± 0.07 and 1.49 ± 0.15 wt%. These values corresponded well with data obtained from melt inclusions, glass, and bulk-rock analyses from the Canaries and elsewhere as well as a feldspar-liquid hygrometer (Weis et al. 2015). Experiments from the current study, however, clearly show that clinopyroxenes from the same La Palma and El Hierro samples can reach significantly higher water contents under pressure annealing that will have an effect on the calculated magmatic water contents. We use the same approach presented in Weis et al. (2015) to calculate parental magmatic water contents of rehydrated clinopyroxenes from this study. Magmatic water contents for La Palma melts range from 3.96 ± 0.80 to 4.32 ± 0.86 wt% (Table 8). For ankaramite melts from El Hierro values between 2.84 ± 0.56 and 3.88 ± 0.78 wt% H_2O are derived. This is complemented with magmatic

TABLE 8. Calculated primary magmatic water contents

Sample	$[H_2O]_{Cpx}$ after annealing (ppm)	^{a} $^{(IV)}Al^{3+}$	$^a Ca^{2+}$	$lnD_{(Cpx-melt)}$	$D_{(Cpx-melt)}$	$[H_2O]_{Melt}$ (wt%)
T1	912	0.244	0.898	–3.513	0.030	3.06 ± 0.62
T2(2)	874	0.245	0.892	–3.499	0.030	2.89 ± 0.58
T3(3)	1064	0.253	0.893	–3.450	0.032	3.35 ± 0.68
T3(4)	1121	0.253	0.893	–3.450	0.032	3.53 ± 0.70
T4	899	0.239	0.888	–3.537	0.029	3.09 ± 0.62
T4(2)	865	0.239	0.888	–3.537	0.029	2.97 ± 0.60
T4(3)	747	0.239	0.888	–3.537	0.029	2.57 ± 0.52
T4(4)	1015	0.239	0.888	–3.537	0.029	3.49 ± 0.70
T4(5)	1086	0.239	0.888	–3.537	0.029	3.73 ± 0.74
T4(7)	1129	0.239	0.888	–3.537	0.029	3.88 ± 0.78
EH-Ank(2)	668	0.206	0.893	–3.751	0.023	2.84 ± 0.56
EH-Ank(3)	670	0.206	0.893	–3.751	0.023	2.85 ± 0.58
LP1971-B(5)	1180	0.233	0.917	–3.600	0.027	4.32 ± 0.86
LP1971-1(4)	1158	0.241	0.899	–3.532	0.029	3.96 ± 0.80
LP1949(5)	998	0.215	0.909	–3.712	0.024	4.08 ± 0.82
MP-4[b]	151	0.096	0.842	–4.416	0.012	1.25 ± 0.24
MP-5[b]	177	0.096	0.842	–4.416	0.012	1.46 ± 0.30
MP-6	794	0.103	0.851	–4.379	0.013	6.34 ± 1.26
MP-7	712	0.092	0.838	–4.440	0.012	6.03 ± 1.20
MP-8	768	0.241	0.907	–3.544	0.029	2.66 ± 0.54

Notes: Calculated uncertainties (2 s.d.) for $^{(IV)}Al^{3+}$ and Ca^{2+} are ±0.010 and ±0.007 for $D_{Cpx-melt}$. Estimated uncertainties for water contents are ±20% for Cpx and magmas.
[a] Average values from Table 2.
[b] Values for $^{(IV)}Al^{3+}$ and Ca^{2+} are based on averages from crystals MP-3, MP-6, and MP-7.

water contents between 1.25 ± 0.24 and 6.34 ± 1.26 wt% H_2O for basaltic andesite from Merapi.

The values for magmatic water contents for the La Palma melts are considerably higher than those determined by Weis et al. (2015) (0.71 ± 0.07 to 1.49 ± 0.15 wt% H_2O) and are more similar to melts from El Hierro's Tanganasoga volcano (2.84 ± 0.56 to 3.88 ± 0.78 wt% H_2O) (Table 6). This overlap is expected considering that both islands are part of the Western Canaries and that Tanganasoga melts can be seen as the volatile-rich primitive magma source in the upper mantle (e.g., Manconi et al. 2009). Magmatic water contents for ankaramite magmas from Teno volcano on Tenerife, a volcanic system similar to Tanganasoga, have been estimated to have been up to 3 wt% (Longpré et al. 2009b; Fig. 8) supporting the high values obtained through pressure-annealed clinopyroxenes. In addition, magmatic water contents for the Western Canaries can be estimated using compositional data of amphibole and the thermobarometric formulations by Ridolfi and Renzulli (2012) (Eqs. 1a and 4). Using compositional data for amphibole pheno- and xenocrysts in basanite and phonolite lavas from La Palma and the kaersutite cumulate xenolith from this study (sample LP1971-B) (Klügel et al. 2000; Barker et al. 2015) reveals magmatic water contents between 3.37 ± 0.78 and 4.48 ± 0.78 wt% H_2O (Appendix[1] A1) with an average of 3.76 ± 0.78 wt% H_2O. These values overlap with the range obtained through pressure-annealed clinopyroxene from the Western Canaries. Most amphibole crystals in the 1971 lavas on La Palma are xenocrysts; however, amphibole in the Western Canaries crystallizes at the same depth as the clinopyroxene (20–45 km) (Klügel et al. 2005; Longpré et al. 2009a; Barker et al. 2015; Weis et al. 2015). Thus the xenocrysts provide a guideline for the H_2O content in the volcanic system at this depth. Furthermore, the values obtained from amphibole phenocrysts in phonotephrites (3.47 ± 0.78 to 4.48 ± 0.78 wt% H_2O) from the 1949 eruption

on La Palma (Klügel et al. 2000) provide a direct comparison for magmatic water contents at depth. Amphibole from sample LB1971-B reveals magmatic water contents between 3.25 ± 0.78 and 4.17 ± 0.78 wt% while pressure-annealed clinpyroxene revealed 4.32 ± 0.86 wt% H_2O. The available melt inclusion and volcanic glass data for the Canaries and other ocean island basalts correspond to entrapment pressures between 0.3 and 0.5 kbar (e.g., Dixon et al. 1997; Wallace 1998), which are far below the crystallization pressures of Western Canary clinopyroxene (cf. Klügel et al. 2005; Longpré et al. 2009a; Barker et al. 2015; Weis et al. 2015). Thus the melt inclusions and water contents in clinopyroxene annealed at 1 atm may represent the water contents in the upper parts of the volcanic system after potential H_2O loss from the magma while pressure-annealed clinopyroxenes most likely represent the undegassed magmatic water content at crystallization in the upper mantle.

Similar to the results from the Canaries, are the results for Merapi volcano. Merapi clinopyroxenes rehydrated at 1 atm reveal magmatic water contents of 1.25 ± 0.24 and 1.46 ± 0.30 wt%. These values overlap with melt inclusion data reported in the literature (Gertisser 2001; Nadeau et al. 2013; Preece et al. 2014; Fig. 8). Most melt inclusions from Merapi are considered to have undergone H_2O loss (Gertisser 2001; Preece et al. 2014), to be re-equilibrated (Preece et al. 2014) or to be of secondary origin (Nadeau et al. 2013). Entrapment and re-equilibration of the melt inclusions occurred at depth between 0.6 and 9.7 km (Nadeau et al. 2013; Preece et al. 2014). Pressure-annealed clinopyroxene phenocrysts, however, reveal magmatic water contents around 6.0 ± 1.2 wt% that overlap with magmatic H_2O contents determined through amphibole in the lava samples (~6.0 ± 0.9 wt% H_2O; Costa et al. 2013; Nadeau et al. 2013). Crystallization of host clinopyroxene and amphibole occurred much deeper in the volcanic system between 14 and 25 km (Gertisser 2001; Chadwick et al. 2013; Costa et al. 2013; Nadeau et al. 2013; Preece et al. 2014). Furthermore, the clinopyroxene-based magmatic water contents fall within the range of water contents for vapor-saturated basaltic andesite at depths between 14 and 25 km (6 to 10 wt% H_2O) (Pineau et al. 1998). The magmatic water content of 2.66 ± 0.54 wt% determined by crystal MP-8, annealed at 0.5 kbar, lies within range of values determined by melt inclusions. Together with clinopyroxene annealed at 1 atm this sample represents the magmatic water contents in the shallower part of the volcanic system after various stages of magma degassing. Phenocrysts annealed at higher pressure, on the contrary, are representative for magmatic water contents at the depth of their crystallization and prior to degassing.

One problem with comparing the clinopyroxene data to magmatic water contents derived by amphibole is the timing of crystallization. NAMs and in this case clinopyroxene usually crystallize earlier than amphibole. Significant fractionation of NAMs thus might enrich the residual melt in H_2O that then leads to the onset of amphibole crystallization. Thus the comparison of the two minerals might actually indicate an excessive rehydration of the crystals. However, especially for Merapi, modeling showed that amphibole and clinopyroxene crystallization occurred simultaneously (e.g., Costa et al. 2013). Most Merapi clinopyroxenes in this study are low in Al_2O_3 (Table 2). The low-Al clinopyroxene has been determined by thermobarometry and modeling to
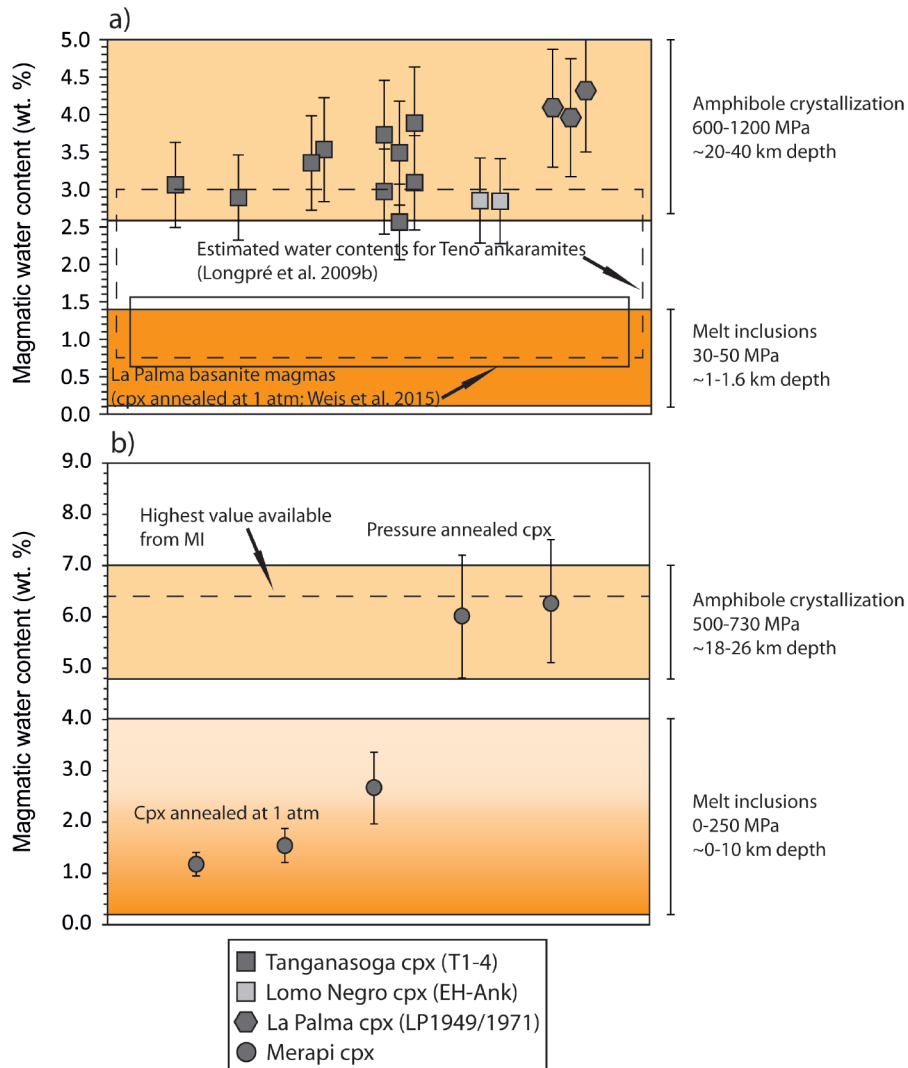
FIGURE 8. Distribution of calculated water contents for parental melts of clinopyroxene from (**a**) El Hierro and La Palma and (**b**) Merapi volcano. Magma H_2O contents calculated on the basis of pressure-annealed clinopyroxenes from the Western Canaries and Merapi correlate well with magmatic water contents at greater depth for these volcanic systems derived through amphiboles. Clinopyroxenes annealed at 1 atm in hydrogen, on the contrary, overlap more with melt inclusion data that represent more the upper part of these volcanic systems. The color gradient in the box indicates the frequency of magmatic water contents derived through Merapi melt inclusions.

have crystallized in the main magma storage level between 10 and 20 km depth (300 to 600 MPa) together with amphibole and plagioclase at magmatic water contents between 4 and 6 wt% (Chadwick et al. 2013; Costa et al. 2013; Nadeau et al. 2013). Amphibole and high-Al clinopyroxene crystallization already commences at deeper levels (Costa et al. 2013). Results from plagioclase-melt hygrometry indicate magmatic water content of 5.0 ± 0.5 wt% in the main magma storage zone (Surono et al. 2012). Thus the comparison of magmatic water contents derived through amphibole and clinopyroxene seems applicable. However, it remains difficult to establish similar relations between clinopyroxene and amphibole for the samples from the Canary Islands. The phonotephrites of the 1949 eruption are seen as a

separate magma batch compared to the basanites (Klügel et al. 2000). Also crystals of both minerals in the kaersutite cumulate sample LP1971-B were accumulated from the same magma, but it is not known if they actually crystallized simultaneously (Barker et al. 2015). Similar, feldspar hygrometry from the La Palma basanites indicates a water content of around 4 wt% in the magma, but crystallization most likely occurred after clinopyroxene (Barker et al. 2015). However, the three independent methods all point toward water contents between 3 and 4 wt%. Furthermore, the highest water contents among untreated clinopyroxene crystals from Tanganasoga would result in magmatic water contents close to 3 wt% and again overlap with values derived through rehydrated crystals. As outlined above, dehy-

dration of the Tanganasoga crystals upon magma degassing and eruption cannot be excluded, which would indicate even higher magmatic water contents at depth.

It cannot be claimed with entire certainty that our rehydration experiments reconstructed the actual initial water contents of clinopyroxenes prior to possible dehydration. However, our results outlined above indicate that it is likely the case.

IMPLICATIONS

The rehydration experiments conducted in this study imply that clinopyroxene crystals begin to dehydrate upon magma ascent within a volcanic system. This dehydration is a consequence of the decrease in pressure with vicinity to the surface and the adaption of the crystals to the new conditions. Furthermore, the crystals may undergo dehydration through oxidation during the eruption and eventually may fully dehydrate. Both types of dehydration occur according to redox-reaction 1. Thus the water content of erupted clinopyroxene phenocrysts cannot be taken for granted as a proxy for magmatic or mantle water contents. The pressure- and oxidation-related dehydration may be hindered by fast magma ascent with minimal magma degassing and more violent eruptions that subsequently lead to quenching of the erupted crystals. In this way the initial water content at crystallization may be preserved to large extents. To reach a rehydration, corresponding to the water content at crystallization, of dehydrated clinopyroxene phenocrysts, experiments at 1 atm in hydrogen gas are not sufficient. It requires the input of pressure to restore water contents of clinopyroxene in the mantle. A precise threshold value for pressure at which the water content in clinopyroxene will be held stable has not been established. Further investigation of rehydration at different pressures in comparison with detailed studies on the crystals' origin and eruption history could help to establish a more precise relation between pressure and clinopyroxene water content. The rehydration at different pressures of dehydrated clinopyroxene phenocrysts from lava samples seems to be able to serve as a proxy for magmatic water contents at different levels in a volcanic system. Thus different pressure experiments could be used to investigate the degassing history of magma in a volcanic system that, in turn, has implications on petrological processes.

REFERENCES CITED

Barker, A.K., Troll, V.R., Carracedo, J.-C. and Nicholls, P.A. (2015) The magma plumbing system for the 1971 Tenguía eruption, La Palma, Canary Islands. Contributions to Mineralogy and Petrology, 170, 54, doi:10.1007/s00410-015-1207-7.

Bell, D.R., Ihinger, P.D., and Rossman, G.R. (1995) Quantitative analysis of trace OH in garnet and pyroxenes. American Mineralogist, 80, 465–474.

Beran, A. (1976) Messung des Ultrarot-Pleochroismus von Mineralen. XIV. Der Pleochroismus der OH-Streckfrequenz in Diopsid. Tschermaks Mineralogische und Petrographische Mitteilungen, 23, 79–85.

Brändle, J.L., Fernandez Santin, S., and Lopez Ruiz, J. (1974) Mineralogy of the materials from Teneguía Volcano, La Palma, Canary Islands. Estudios Geologicos (Madrid), Vol. Teneguía, 41–47.

Bromiley, G.D., Keppler, H., McCammon, C., Bromiley, F.A., and Jacobsen, S.D. (2004) Hydrogen solubility and speciation in natural, gemquality chromian diopside. American Mineralogist, 89, 941–949.

Bunch, T.E., and Reid, A.M. (1975) The nakhlites, part 1: Petrography and mineral chemistry. Meteoritics, 10, 303–315.

Carracedo, J.C., Badiola, E.R., Guillou, H., de La Nuez, J., and Pérez Torrado, F.J. (2001) Geology and volcanology of La Palma and El Hierro, Western Canaries. Estudios Geologicos, 57, 175–273.

Carslaw, H.S., and Jäger, J.C. (1959) Conduction of Heat in Solids. Clarendon Press, Oxford, U.K.

Chadwick, J.P., Troll, V.R., Waight, T.E., van der Zwan, F.M., and Schwarzkopf, L.M. (2013) Petrology and geochemistry of igneous inclusions in recent Merapi deposits: a window into the sub-volcanic plumbing system. Contributions to Mineralogy and Petrology, 165, 259–282.

Cherniak, D.J., and Dimanov, A. (2010) Diffusion in pyroxene, mica and amphibole. Reviews in Mineralogy and Geochemistry, 72, 641–690.

Costa, F., Supriyati, A., Bouvet de Maisonneuve, C., and Pallister, J.S. (2013) Petrological insights into the storage conditions, and magmatic processes that yielded the centennial 2010 Merapi explosive eruption. Journal of Volcanology and Geothermal Research, 262, 209–235.

Dixon, J.E., Clague, D.A., Wallace, P., and Poreda, R. (1997) Volatiles in alcalic basalts from the North Arch Volcanic Field, Hawaii: extensive degassing of deep submarine-erupted alkali series lavas. Journal of Petrology, 38, 911–939.

Dyar, M.D. (2003) Ferric iron in SNC meteorites as determined by Mössbauer spectroscopy: Implications for martian landers and martian oxygen fugacity. Meteoritics and Planetary Science, 38, 1733–1752.

Farver, J.R. (2010) Oxygen and hydrogen diffusion in minerals. Reviews in Mineralogy and Geochemistry, 72, 447–507.

Gertisser, R. (2001) Gunung Merapi (Java, Indonesien): Eruptionsgeschichte und magmatische Evolution eines Hochrisiko-Vulkans, 394 p. Ph.D. thesis, Universität Freiburg (in German).

Gustafson, W.I. (1974) The stability of andradite, hedenbergite, and related minerlas in the system Ca-Fe-Si-O-H. Journal of Petrology, 15, 455–496.

Hamada, M., Kawamoto, T., Takahashi, E., and Fujii, T. (2011) Polybaric degassing of island arc low-K tholeiitic basalt magma recorded by OH concentrations in Ca-rich plagioclase. Earth and Planetary Science Letters, 308, 259–266.

Harvey, J., Yoshikawa, M., Hammond, S.J., and Burton, K.W. (2012) Deciphering the trace element characteristics in Kilbourne Hole peridotite xenoliths: melt-rock interaction and metasomatism beneath the Rio Grande Rift, SW USA. Journal of Petrology, 53, 1709–1742.

Hercule, S., and Ingrin, J. (1999) Hydrogen in diopsides: Diffusion, kinetics of extraction-incorporation, and solubility. American Mineralogist, 84, 1577–1587.

Ingrin, J., and Blanchard, M. (2006) Diffusion of hydrogen in minerals. Reviews in Mineralogy and Geochemistry, 62, 291–320.

Ingrin, J., and Skogby, H. (2000) Hydrogen in nominally anhydrous upper-mantle minerals: Concentration levels and implications. European Journal of Mineralogy, 12, 543–570.

Ingrin, J., Hercule, S., and Charton, T. (1995) Diffusion of hydrogen in diopside: Results of dehydration experiments. Journal of Geophysical Research, 100, 489–499.

Kil, Y., and Wendlandt, R.F. (2004) Pressure and temperature evolution of upper mantle under the Rio Grande rift. Contributions to Mineralogy and Petrology, 148, 2665–2680.

Klügel, A., Hoernle, K.A., Schmincke, H.-U., and White, J.D.L. (2000) The chemically zoned 1949 eruption on La Palma (Canary Islands): Petrologic evolution and magma supply dynamics of a rift zone eruption. Journal of Geophysical Research, 105, 5997–6016.

Klügel, A., Hansteen, T.H., and Galipp, K. (2005) Magma storage and underplating beneath Cumbre Vieja volcano, La Palma (Canary Islands). Earth and Planetary Science Letters, 236, 211–226.

Koch-Müller, M., Abs-Wurmbach, I., Rhede, D., Kahlenberg, V., and Matsyuk, S. (2007) Dehydration experiments on natural omphacites: qualitative and quantitative characterization by various spectroscopic methods. Physics and Chemistry of Minerals, 34, 663–678.

Kovács, I., Green, D.H., Rosenthal, A., Hermann, J., O'Neill, H.St.C., Hibberson, W.O., and Udvardi, B. (2012) An experimental study of water in nominally anhydrous minerals in the upper mantle near the water-saturated solidus. Journal of Petrology, 53, 2067–2093.

Libowitzky, E., and Rossman, G.R. (1997) An IR absorption calibration for water in minerals. American Mineralogist, 82, 1111–1115.

Lloyd, A.S. (2014) Timescales of magma ascent during explosive eruptions: Insights from the re-equilibration of magmatic volatiles, 176 p. Ph.D. thesis, Columbia University, New York.

Longpré, M.-A., Troll, V.R., and Hansteen, T.H. (2008) Upper mantle magma storage and transport under a Canarian shield-volcano, Teno, Tenerife (Spain). Journal of Geophysical Research, 113, B08203, doi:10.1029/2007JB005422.

Longpré, M.A., Troll, V.R., Hansteen, T.H., and Anderson, E. (2009a) Ankaramitic Lavas and Clinopyroxene Megacrysts from the Tanganasoga Volcano, El Hierro Island (Canary Archipelago). Eos Transactions AGU, 90(52), Fall Meeting Supplement, Abstract V51A-1662.

Longpré, M.A., Troll, V.R., Walter, T.R., and Hansteen, T.H. (2009b) Volcanic and geochemical evolution of the Teno massif, Tenerife, Canary Islands: Some repercussions on giant landslides on ocean island magmatism. Geochemistry Geophysics Geosystems, 10, Q12017, doi:10.1029/2009GC002892.

Manconi, A., Longpré, M.A., Walter, T.R., Troll, V.R., and Hansteen, T.H. (2009) The effects of flank collapses on volcano plumbing systems. Geology, 37, 1099–1102.

Morimoto, N., Fabries, J., Ferguson, A.K., Ginzburg, I.V., Ross, M., Seifert, F.A., Zussman, J., Aoki, K., and Gottardi, G. (1988) Nomenclature of pyroxenes. American Mineralogist, 73, 1123–1133.

Mosenfelder, J., and Rossman, G.R. (2013) Analysis of hydrogen and fluorine in pyroxenes: II. Clinopyroxene. American Mineralogist, 98, 1042–1054.

Nadeau, O., Williams-Jones, A.E., and Stix, J. (2013) Magmatic-hydrothermal evolution and devolatilization beneath Merapi volcano, Indonesia. Journal of Volcanology and Geothermal Research, 261, 50–68.

Nazzareni, S., Skogby, H., and Zanazzi, P.F. (2011) Hydrogen content in clinopyroxene phenocrysts from Salina mafic lavas (Aeolian arc, Italy). Contributions to Mineralogy and Petrology, 162, 275–288.

Okumura, S. (2011) The H_2O content of andesitic magmas from three volcanoes in Japan, inferred from the infrared analysis of clinopyroxene. European Journal of Mineralogy, 23, 771–778.

O'Leary, J.A., Gaetani, G.A., and Hauri, E.H. (2010) The effect of tetrahedral Al^{3+} on the partitioning of water between clinopyroxene and silicate melt. Earth and Planetary Science Letters, 297, 111–120.

Pedrazzi, D., Becerril, L., Martí, J., Meletlidis, S., and Galindo, I. (2014) Explosive felsic volcanism on El Hierro (Canary Islands). Bulletin of Volcanology, 76, 863.

Pineau, F., Shilobreeva, S., Kadik, A., and Javoy, M. (1998) Water solubility and D/H fractionation in the system basaltic andesite-H_2O at 1250°C and between 0.5 and 3 kbars. Chemical Geology, 147, 173–184.

Pinel, V., and Jaupart, C. (2000) The effect of edifice load on magma ascent beneath a volcano. Philosophical Transactions of the Royal Society A—Mathematical, Physical and Engineering Sciences, 358, 1515–1532.

Pitzer, K.S., and Sterner, S.M. (1994) Equation of state valid continuously from zero to extrem pressures for H_2O and CO_2. Journal of Chemical Physics, 101, 3111–3116.

Preece, K., Gertisser, R., Barclay, J., Berlo, K., and Herd, R.A. (2014) Pre- and syn-eruptive degassing and crystallisation processes of the 2010 and 2006 eruptions of Merapi volcano, Indonesia. Contributions to Mineralogy and Petrology, 168, 1061.

Prescher, C., McCammon, C., and Dubrovinsky, L. (2012) MossA: a program for analyzing energy-domain Mössbauer spectra from conventional and synchrotron sources. Journal of Applied Crystallography, 45, 329–331.

Purwin, H., Stalder, R., and Skogby, H. (2009) Hydrogen incorporation in Fe- and Na-doped diopsides. European Journal of Mineralogy, 21, 691–704.

Ratdomopurbo, A., Beauducel, F., Subandriyo, J., Made Agung Nandaka, I.G., Newhall, C.G., Sayudi, D.S., and Suparwaka, H. (2013) Overview of the 2006 eruption of Mt. Merapi. Journal of Volcanology and Geothermal Research, 261, 87–97.

Ridolfi, F., and Renzulli, A. (2012) Calcic amphiboles in calc-alkaline and alkaline magmas: thermobarometric and chemometric empirical equations valid up to 1130 °C and 2.2 GPa. Contributions to Mineralogy and Petrology, 163, 877–895.

Skogby, H. (1994) OH incorporation in synthetic clinopyroxenes. American Mineralogist, 79, 240–249.

——— (2006) Water in natural mantle minerals I: Pyroxenes. Reviews in Mineralogy and Geochemistry, 62, 155–168.

Skogby, H., and Rossman, G.R. (1989) OH- in pyroxene: an experimental study of incorporation mechanisms and stability. American Mineralogist, 74, 1059–1069.

Stalder, R. (2004) Influence of Fe, Cr and Al on hydrogen incorporation in orthopyroxene. European Journal of Mineralogy, 16, 703–711.

Stalder, R., and Ludwig, T. (2007) OH incorporation in synthetic diopside. European Journal of Mineralogy, 19, 373–380.

Stalder, R., and Skogby, H. (2003) Hydrogen diffusion in natural and synthetic orthopyroxene. Physics and Chemistry of Minerals, 30, 12–19.

——— (2007) Dehydration mechanisms in synthetic Fe-bearing enstatite. European Journal of Mineralogy, 19, 201–216.

Stalder, R., Kronz, A., and Simon, K. (2008) Hydrogen incorporation in enstatite in the system MgO-SiO_2-H_2O-$NaCl$. Contributions to Mineralogy and Petrology, 156, 653–659.

Stroncik, N.A., Klügel, A., and Hansteen, T.H. (2009) The magmatic plumbing system beneath El Hierro (Canary Islands): constraints from phenocrysts and naturally quenched basaltic glasses in submarine rocks. Contributions to Mineralogy and Petrology, 157, 593–607.

Sundvall, R., and Skogby, H. (2011) Hydrogen defect saturation in natural pyroxene. Physics and Chemistry of Minerals, 38, 335–344.

Sundvall, R., and Stalder, R. (2011) Water in upper mantle pyroxene megacrysts and xenocrysts: A survey study. American Mineralogist, 96, 1215–1227.

Sundvall, R., Skogby, H., and Stalder, R. (2009) Dehydration-hydration mechanisms in synthetic Fe-poor diopside. European Journal of Mineralogy, 21, 17–26.

Surono, J.P., Pallister, J., Boichu, M., Buongiorno, M.F., Budisantoso, A., Costa, F., Andreastuti, S., Prata, F., Schneider, D., Clarisse, L., and others. (2012) The 2010 explosive eruption of Java's Merapi volcano—a '100-year' event. Journal of Volcanology and Geothermal Research, 241-242, 121–135.

Troll, V.R., Deegan, F.M., Jolis, E.M., Harris, C., Chadwick, J.P., Gertisser, R., Schwarzkopf, L.M., Borisova, A.Y., Bindeman, I.N., Sumarti, S., and Preece, K. (2013) Magmatic differentiation process at Merapi Volcano: Inclusion petrology and oxygen isotopes. Journal of Volcanology and Geothermal Research, 261, 38–49.

Treiman, A.H. (1993) The parent magma of the Nakhla (SNC) meteorite, inferred from magmatic inclusions. Geochimica et Cosmochimica Acta, 57, 4753–4767.

Villasante-Marcos, V., and Pavón-Carrasco, F.J. (2014) Palaeomagnetic constraints on the age of Lomo Negro volcanic eruption (El Hierro, Canary Islands). Geophysical Journal International, 199, 1497–1514.

Wade, J.A., Plank, T., Hauri, E.H., Kelley, K.A., Roggensack, K., and Zimmer, M. (2008) Prediction of magmatic water contents via measurement of H_2O in clinopyroxene phenocrysts. Geology, 36, 799–802.

Wallace, P.J. (1998) Pre-eruptive H_2O and CO_2 contents of mafic magmas from the submarine to emergent shield stages of Gran Canaria. In P.P.E. Weaver, H.-U. Schmincke, J.V. Firth, and W. Duffield, Eds., Proceedings of the Ocean Drilling Program, Scientific Results, 157, p. 411–420.

Weis, F.A., Skogby, H., Troll, V.R., Deegan, F.M., and Darehn, B. (2015) Magmatic water contents determined through clinopyroxene: Examples from the Western Canary Islands, Spain. Geochemistry, Geophysics, Geosystems, 16, 2127–2146.

Woods, S.C., Mackwell, S., and Dyar, D. (2000) Hydrogen in diopside: Diffusion profiles. American Mineralogist, 85, 480–487.

Xia, Q.K., Liu, J., Liu, S., Kovacs, I., Feng, M., and Dang, L. (2013) High water content in Mesozoic primitive basalts of the North China Craton and implications on the destruction of cratonic mantle lithosphere. Earth and Planetary Science Letters, 36, 85–97.

Xirouchakis, D., and Lindsley, D.H. (1998) Equilibria among titanite, hedenbergite, fayalite, quartz, ilmenite, and magnetite: Experiments and internally consistent thermodynamic data for titanite. American Mineralogist, 83, 712–725.

Yang, X., Liu, D., and Xia, Q. (2014) CO_2-induced small water solubility in olivine and implications for properties of the shallow mantle. Earth and Planetary Science Letters, 403, 37–47.